RESEARCH ARTICLE SUMMARY

AGING

Counteracting age-related VEGF signaling insufficiency promotes healthy aging and extends life span

M. Grunewald*, S. Kumar†, H. Sharife†, E. Volinsky†, A. Gileles-Hillel, T. Licht, A. Permyakova, L. Hinden, S. Azar, Y. Friedmann, P. Kupetz, R. Tzuberi, A. Anisimov, K. Alitalo, M. Horwitz, S. Leebhoff, O. Z. Khoma, R. Hlushchuk, V. Djonov, R. Abramovitch, J. Tam, E. Keshet*

INTRODUCTION: All body cells rely on blood vessels (BVs) for the provision of oxygen and other blood-borne substances and, in certain settings, also for the provision of endothelial-derived paracrine factors. Like other organ systems, the vascular system undergoes aging, which leads to progressive functional deterioration. Given the centrality of BVs to organ homeostasis, it has been hypothesized that vascular aging is an upstream, founding factor in organismal aging, but experimental support for this proposition is limited. Vascular aging involves both large and small vessels, with the latter marked by capillary rarefaction, i.e., age-related failure to maintain adequate microvascular density (MVD). A key homeostatic mechanism preventing MVD reduction relies on the angiogenic activity of vascular endothelial growth factor (VEGF), which by virtue of its hypoxic inducibility, constantly acts to replenish lost vessels and match vascular supply to the tissue needs. The reason(s) that VEGF fails to do so during aging is unknown.

RATIONALE: Compromised vascular function is expected to perturb organ homeostasis in ways conducive for the development of age-related frailties and diseases. Accordingly, counteracting critical facets of vascular aging might be a useful approach for their alleviation. The presumption that insufficient vascular supply in aging is underlined by VEGF signaling insufficiency, primarily (but not exclusively) because of its indispensable role in preventing capillary loss, led us to investigate whether securing a young-like level of VEGF signaling might rectify capillary loss and its sequelae. On the premise that deteriorated vascular function is an upstream driver of multiorgan malfunctioning, it is envisioned that its rectification might confer comprehensive geroprotection.

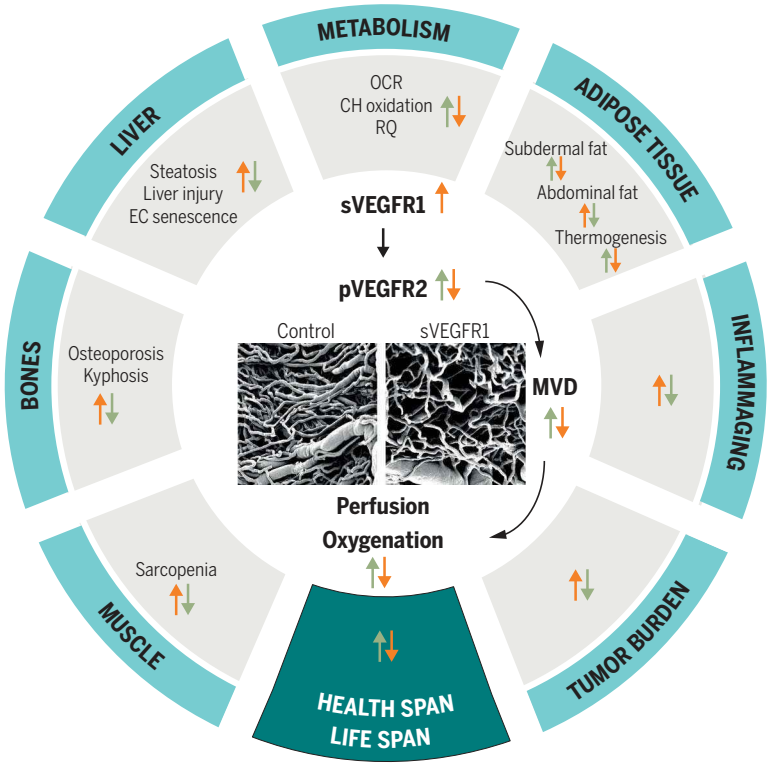

Centrality of VEGF and vascular alterations in age-related phenotypes. Shown is a graphic representation of age-associated alterations in organ physiology and function (orange arrows) alleviated by VEGF gain of function (green arrows). Insert shows vascular casts of a native adult mouse myocardium before (control) and after sVEGFR1 induction, highlighting a failure to maintain adequate MVD in the presence of impaired VEGF signaling, a process that takes place naturally during aging. OCR, oxygen consumption rate; CH, carbohydrate; RQ, respiratory quotient; pVEGFR2: phosphorylated VEGFR2.

RESULTS: Although VEGF production is not significantly reduced during mouse aging, longitudinal monitoring revealed that VEGF signaling was greatly reduced in multiple key organs. This was associated with increased production of soluble VEGFR1 (sVEGFR1) generated through an age-related shift in alternative splicing of VEGFR1 mRNA and its activity as a VEGF trap. A modest increase of circulatory VEGF using a transgenic VEGF gain-of-function system or adeno-associated virus (AAV)–assisted VEGF transduction maintained a more youthful level of VEGF signaling and provided protection from age-related capillary loss, compromised perfusion, and reduced tissue oxygenation. Aging hallmarks such as mitochondrial dysfunction, compromised metabolic flexibility, endothelial cell senescence, and inflammaging were alleviated in VEGF-treated mice. Conversely, VEGF loss of function by conditional induction of transgenic sFlt1 in endothelial cells accelerated the development of these adverse age-related phenotypes. VEGF-treated mice lived longer and had an extended health span, as reflected by reduced abdominal fat accumulation, reduced liver steatosis, reduced muscle loss (sarcopenia) associated with better preservation of muscle-generating force, reduced bone loss (osteoporosis), reduced kyphosis, and reduced burden of spontaneous tumors.

CONCLUSION: The study provides compelling evidence for the proposition that vascular aging is a hierarchically high driver of overall organismal aging. It places VEGF signaling insufficiency at center stage to multiorgan aging and suggests that its undoing might confer comprehensive geroprotection. ■

The list of author affiliations is available in the full article online.
*Corresponding author. Email: myriamg@ekmd.huji.ac.il (M.G.); elik@ekmd.huji.ac.il (E.K.)
†These authors contributed equally to this work.
Cite this article as M. Grunewald *et al.*, *Science* **373**, eabc8479 (2021). DOI: 10.1126/science.abc8479

READ THE FULL ARTICLE AT
https://doi.org/10.1126/science.abc8479

RESEARCH ARTICLE

AGING

Counteracting age-related VEGF signaling insufficiency promotes healthy aging and extends life span

M. Grunewald[1]*, S. Kumar[1]†, H. Sharife[1]†, E. Volinsky[1]†, A. Gileles-Hillel[1,2,3], T. Licht[1], A. Permyakova[4], L. Hinden[4], S. Azar[4], Y. Friedmann[5], P. Kupetz[1], R. Tzuberi[1], A. Anisimov[6], K. Alitalo[6], M. Horwitz[1], S. Leebhoff[1], O. Z. Khoma[7], R. Hlushchuk[7], V. Djonov[7], R. Abramovitch[2], J. Tam[4], E. Keshet[1]*

Aging is an established risk factor for vascular diseases, but vascular aging itself may contribute to the progressive deterioration of organ function. Here, we show in aged mice that vascular endothelial growth factor (VEGF) signaling insufficiency, which is caused by increased production of decoy receptors, may drive physiological aging across multiple organ systems. Increasing VEGF signaling prevented age-associated capillary loss, improved organ perfusion and function, and extended life span. Healthier aging was evidenced by favorable metabolism and body composition and amelioration of aging-associated pathologies including hepatic steatosis, sarcopenia, osteoporosis, "inflammaging" (age-related multiorgan chronic inflammation), and increased tumor burden. These results indicate that VEGF signaling insufficiency affects organ aging in mice and suggest that modulating this pathway may result in increased mammalian life span and improved overall health.

The vascular system is the largest cellular network that is shared by all organs. All cells in our body depend on blood vessels (BVs) for the provision of oxygen and other blood-borne substances, waste removal, and supply of essential angiocrine factors secreted by endothelial cells (ECs) (*1*). Like other organ systems, BVs undergo aging that is associated with reduced functionality (*2*). Therefore, age-related loss of vascular function is likely to affect organ physiology, prompting a "vascular theory of aging" (*3*), i.e., the proposition that vascular aging is a high driver of aging, but experimental proof is limited.

Pathologies affecting the arteries, which include arterial stiffening, atherosclerosis, and other vascular occlusive events, lead to a host of cardiovascular diseases (CVDs) the prevalence of which increases with age (*4*). The most substantial age-related process affecting capillaries in all organs is a progressive reduction in microvascular density (MVD), a phenomenon known as microvascular rarefaction (*2*, *5*). Alleviation or aggravation of age-associated pathologies other than "classical" CVDs by vascular manipulation have been demonstrated in a few animal studies (*6*–*11*).

Vascular endothelial growth factor (VEGF) is a highly pleiotropic growth factor with both vascular and nonvascular functions (*12*). In addition to its angiogenic activity, VEGF plays essential roles in controlling vascular permeability, sustaining the survival of newly formed BVs, maintaining organ-specific vascular traits such as the formation and maintenance of capillary fenestrations and other EC barrier functions, and the induction of certain organ-specific angiocrine factors (*1*). VEGF can be produced in many adult tissues, and its cognate receptors, which are expressed in ECs and in a host of nonvascular cells, are often constitutively phosphorylated, suggesting active VEGF signaling (*13*). Because it is induced by hypoxia, VEGF constantly acts and is indispensable in matching MVD to changes in tissue needs (*14*). Previous studies have shown that age-dependent decline of hippocampal neurogenesis (*15*), liver regeneration (*16*), and skeletal muscle exercise capacity (*8*) can be alleviated by improved VEGF signaling. In this study, we investigated whether counteracting age-related impairment of VEGF signaling may confer comprehensive geroprotection.

Maintenance of VEGF signaling in aged mice prevents microvascular rarefaction and improves tissue perfusion and oxygenation

To determine whether the failure to maintain adequate MVD in aging is caused by insufficient VEGF signaling, we investigated whether securing a young-like level of VEGF signaling through a compensatory, mild increase of systemic VEGF levels might prevent microvascular rarefaction and its adverse sequelae. A bi-transgenic "Tet-off" mouse platform was used in which transgenic VEGF produced by hepatocytes is continuously released into the systemic circulation and is accessible to all peripheral tissues (see the supplementary materials and methods for a description of the Tet-off system used). Circulating VEGF levels in these mice (designated "VEGF mice") from early to middle adulthood and throughout their life span, are twofold higher than the homeostatic levels of circulatory VEGF (Fig. 1A and fig. S1). All measurements and phenotypes are based on pairwise comparisons of VEGF mice and littermate controls maintained under identical conditions. Serving as controls were littermates that inherited only one of the two transgenes required for transgenic VEGF induction, thus arguing against possible influences exerted by transgene integration sites.

In control mice, systemic VEGF levels and VEGF levels in major peripheral organs (fig. S2) did not significantly decrease with age in most examined organs. To determine the status of VEGF signaling in aging, we measured relative levels of VEGF receptor 2 (VEGFR2) phosphorylation of tyrosine 1175, a site shown to be essential for VEGF-promoted EC proliferation (*17*). VEGF signaling was compromised in 24-month-old (Mo) control mice but not in VEGF mice littermates, which maintained a young-like level of VEGFR2 phosphorylation not just in the liver (the organ from which transgenic VEGF emanates) but also in remote organs, as represented here by hindlimb muscle (Fig. 1B).

To understand the discordance between VEGF protein and VEGF signaling levels in aging, we investigated whether natural decoy receptors such as soluble VEGF receptor 1 (sFlt1) (*18*) might have trapped VEGF (*18*). Longitudinal monitoring revealed progressive buildup of sFlt1 in plasma such that by 1 year of age, sFlt1 levels were already twofold higher than during early adulthood (Fig. 1C). Age-associated increase of sFlt1 expression in the aorta, hepatic central veins, hepatic sinusoidal ECs, and muscle capillaries were identified as the major, albeit not the exclusive, sources of circulatory sFlt1 (Fig. 1D). There was no significant age-associated change in tissue expression of full-length VEGFR1 mRNA (fig. S3). Increased sFlt1 production could be attributed to an age-associated shift in alternative splicing toward increased sFlt1 mRNA production at the expense of mRNA encoding the full-length receptor (Fig. 1E).

To prove a causal relationship between excessive sFlt1 production and reduced VEGF signaling, sFlt1 was conditionally induced in a bi-transgenic Tet-off system composed of an endothelial-specific driver transgene and a sFlt1 responder transgene (mice designated as "sFlt1 mice"). Earlier accumulation of sFlt1 in adult mice to levels comparable to those

[1]Faculty of Medicine, The Hebrew University of Jerusalem, Jerusalem, Israel. [2]Wohl Institute for Translational Medicine and the Goldyne Savad Institute for Gene Therapy, Hadassah Hospital, Jerusalem, Israel. [3]Pediatric Pulmonology and Sleep Unit, Department of Pediatrics, Hadassah Medical Center, Jerusalem, Israel. [4]Obesity and Metabolism Laboratory, Institute for Drug Research, School of Pharmacy, Faculty of Medicine, The Hebrew University, Jerusalem, Israel. [5]Bio-Imaging Unit, The Alexander Silberman Institute of Life Sciences, The Hebrew University, Jerusalem, Israel. [6]Translational Cancer Biology Program, Research Programs Unit, Faculty of Medicine, University of Helsinki, Helsinki, Finland. [7]Topographic and Clinical Anatomy, Institute of Anatomy, University of Bern, Bern, Switzerland.
*Corresponding author. Email: myriamg@ekmd.huji.ac.il (M.G.); elik@ekmd.huji.ac.il (E.K.) †These authors contributed equally to this work.

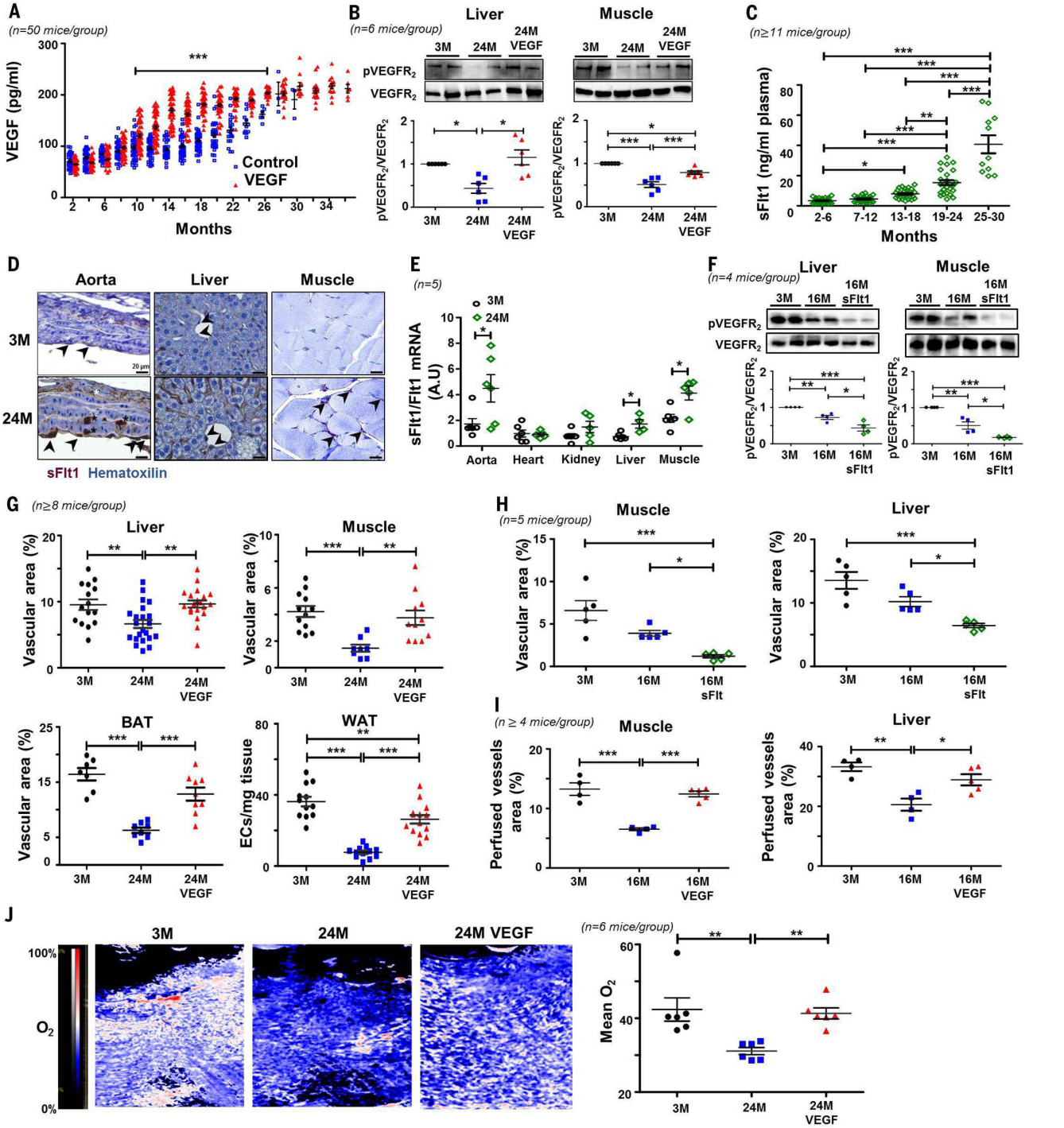

Fig. 1. VEGF signaling is essential to maintaining adequate tissue MVD. (**A**) Plasma VEGF protein levels determined longitudinally in control and VEGF male mice. (**B**) Quantification of the phosphorylated fraction (pVEGFR2: position Y1175) relative to total VEGFR2 in liver and muscle lysates obtained from male mice of the indicated ages. Top: representative immunoblots. Bottom: pVEGFR2/VEGFR2 ratio. (**C**) sFlt1 protein levels in plasma of control mice pooled in the indicated age groups. (**D**) Representative tissue sections of control male mice immunostained with sFlt1-specific antibody and counterstained with hematoxylin and eosin (H&E). Arrowheads indicate sFlt1-positive endothelial cells, white asterisks are sFlt1-positive medial cells, and black asterisks are sFlt1-positive adventitial cells (**E**) sFlt1/Flt1 mRNA ratio in the indicated organs and ages. (**F**) VEGFR2 phosphorylation in liver and muscle of 16 Mo mice in which sFlt1 was induced 8 months earlier. Top: representative immunoblots. Bottom: pVEGFR2/VEGFR2 ratio. (**G**) MVDs in the indicated organs retrieved at the indicated ages and expressed as the relative area covered by $CD31^+$ BVs in the respective tissue sections. For WAT, MVDs are expressed as the number of $CD31^+$ ECs per milligram of tissue as enumerated by flow cytometry. (**H**) MVDs in muscle (left) and liver (right) isolated from sFlt1-induced mice. (**I**) Densities of perfused vessels marked by uptake of intravenously injected fluorescent VE-cadherin antibodies, calculated as the relative area covered by stained capillaries. Each dot represents the average of 10 tissue sections per mouse. (**J**) Blood oxygen saturation levels (sO_2) determined by ultrasound photoacoustics in the hindlimbs of 3 and 24 Mo control and VEGF male and female mice. Left: representative images. Right: quantification of sO_2. Values are shown as mean ± SEM. *P* values were derived from two-way ANOVA and Bonferroni posttests (A); one-way ANOVA and Tukey posttests [(B), (C), and (F) to (J)]; or two-tailed Student's *t* test (E). $^*P < 0.05$; $^{**}P < 0.01$; $^{***}P < 0.001$; *P* values > 0.05 are not indicated.

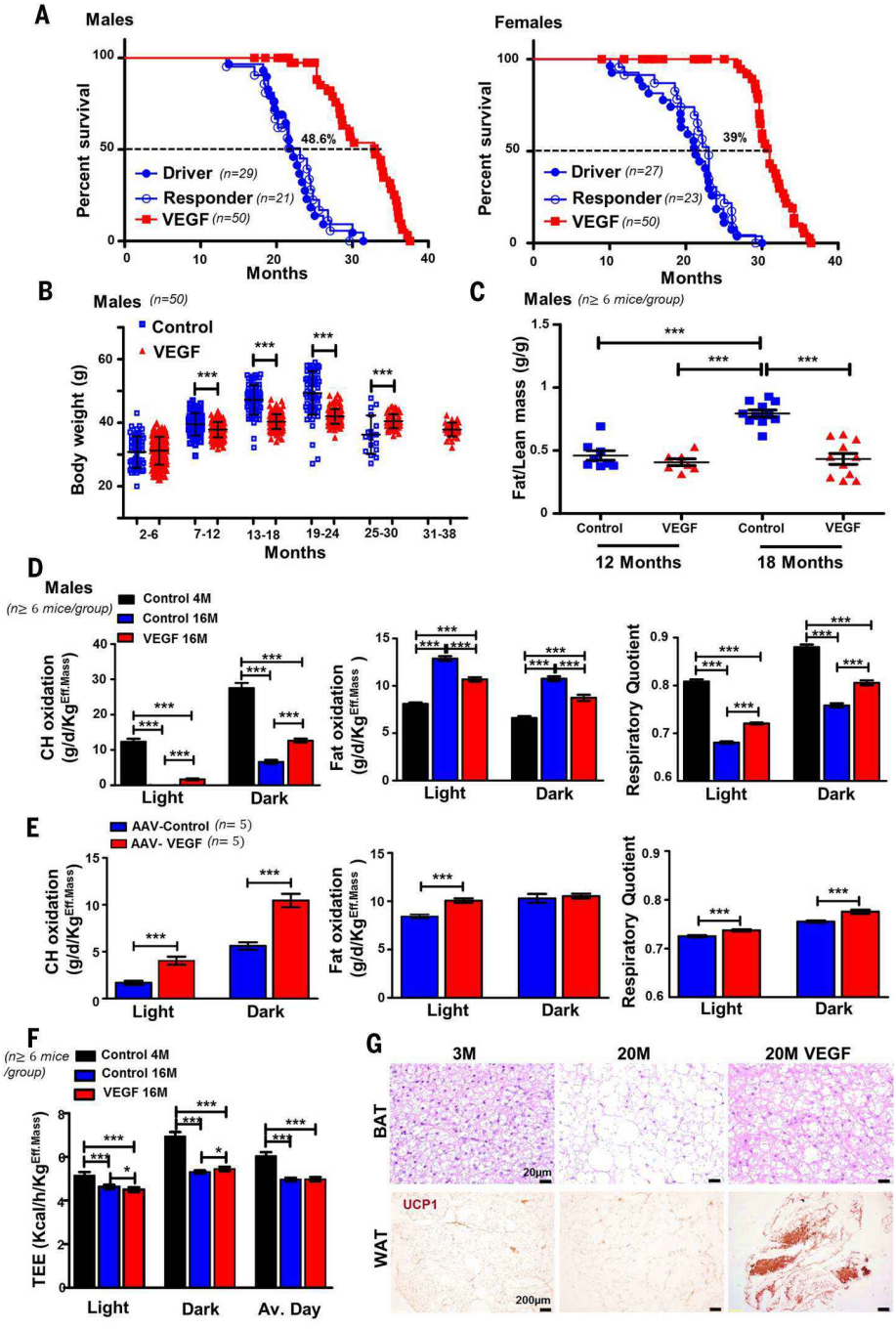

Fig. 2. Increased life span and improved body composition and metabolism of aged VEGF-treated mice. (**A**) Kaplan-Meier survival curves of male and female mice. The control group was subdivided into mice harboring only the driver transgene and mice harboring only the responder transgene. Curves shown also included mice censored for reasons outlined in tables S1 and S2. Percentage indicated is of increased median survival of VEGF mice ($P < 0.0001$). (**B**) Body weights of male mice divided in age groups of 5 to 6 months each. (**C**) Lean-to-fat body mass ratio calculated on the basis of echo-MRI measurements in male mice. (**D**) Circadian changes in carbohydrate (CHO) and fat oxidation (FO) and in RQ individually measured in 4 and 16 Mo male mice. (**E**) Circadian changes in CHO and FO and in RQ in 8 Mo mice infected 6 months earlier with a low titer of AAV-$VEGF_{164}$. Control mice were injected with the same titer of AAV-control. (**F**) TEE of 4 Mo control mice and 16 Mo male controls and VEGF mice normalized to effective body mass. (**G**) Thermogenic brown and beige adipocytes in BAT and WAT. Top: representative H&E–stained BAT sections resected from 3 and 20 Mo mice. Bottom: representative UCP1-immunostained sections of abdominal WAT. Values are shown as mean ± SEM. *P* values were derived from log-rank (Mantel-Cox) test (A); two-tailed unpaired Student's *t* test [(B) and (D) to (F)]; or one-way ANOVA and Tukey posttests (C). $*P < 0.05$; $**P < 0.01$; $***P < 0.001$; *P* values > 0.05 are not indicated.

produced naturally in older mice (fig. S4) resulted in further reduction of VEGF signaling in liver and hindlimb muscle (Fig. 1F).

Microvascular densities in young, old, and old VEGF mice were compared by direct visualization of immunostained BVs in tissue sections and, independently, by flow cytometry–aided EC quantification. We validated a substantial microvascular rarefaction in the liver, muscle, and brown and white adipose tissues of 24 Mo mice. By contrast, microvascular rarefaction was almost fully prevented in age-matched VEGF mice (Fig. 1G and fig. S5). Conversely, experimental VEGF blockade through conditional sFlt1 induction led to accelerated capillary loss, reinforcing a requirement for ongoing VEGF signaling for MVD maintenance (Fig. 1H).

To examine age-associated changes in perfusion, the luminal surfaces of perfused BVs were selectively tagged by intravenously injected, fluorescently labeled vascular endothelial (VE)–cadherin antibodies and subsequently visualized in tissue sections. Reduced perfusion was observed in 16 Mo control mice but not in age-matched VEGF mice, which maintained a young-like level of perfusion (Fig. 1I and fig. S6). Compromised perfusion and its VEGF-aided amelioration were functionally reflected in tissue oxygenation, as measured by ultrasound combined with photoacoustic imaging. The severe reduction in hindlimb muscle oxygenation observed in 24 Mo mice was alleviated in age-matched VEGF mice (Fig. 1J).

VEGF-treated mice have an extended life span and favorable metabolism and body composition

VEGF mice of both sexes displayed an extended median survival and a greater maximal life span compared with their control littermates (Fig. 2A). A litter-by-litter account and levels of circulating

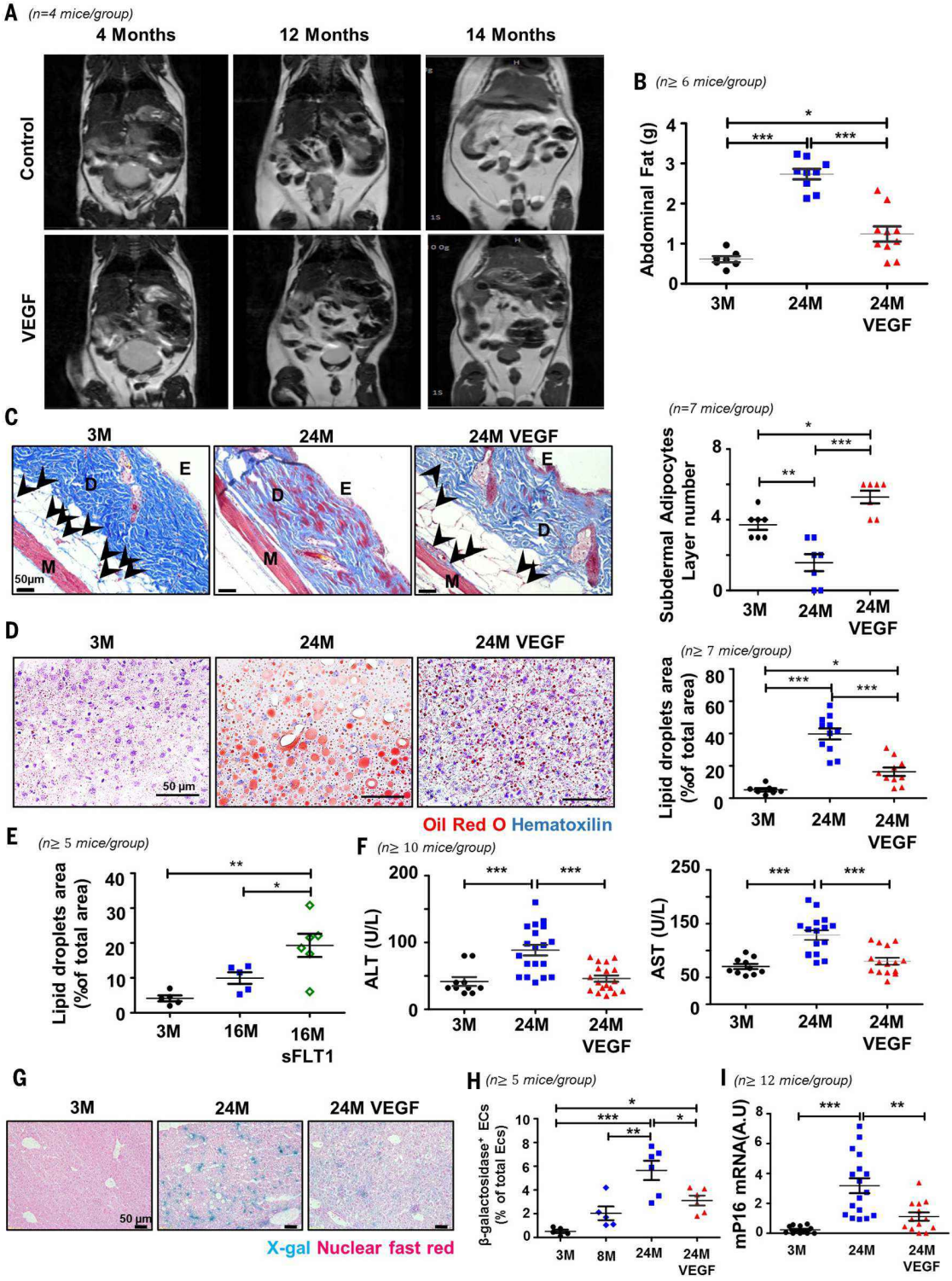

Fig. 3. Age-related alterations in fat distribution and liver pathology negated by VEGF. (**A**) Progressive accumulation of abdominal fat in a representative pair of control and VEGF male mice littermates visualized by MRI (fat appears white). (**B**) Combined weights of epididymal and inguinal fat resected from young and old male mice. (**C**) Left: representative Masson-Trichrome–stained skin sections from 3 and 24 Mo male mice. Arrowheads indicate subdermal capillaries. E, epidermis; D, dermis; M, muscle. Right: number of subdermal adipocyte layers. (**D**) Representative liver sections from 3 and 24 Mo mice stained with Oil Red O and counterstained with H&E. Right: quantification of lipid accumulation in hepatocytes. Each dot represents the average area covered by Oil Red O staining from three to six different sections per mouse. (**E**) Quantification of lipid accumulation in hepatocytes in livers isolated from 3 and 16 Mo control and sFlt1 mice (**F**) Serum levels of the liver enzymes alanine transaminase (ALT) and aspartate transaminase (AST). (**G**) Representative liver cryosections stained for SA-β-gal. (**H**) Fraction of senescent ECs ($Cd45^-Ter119^-CD31^+$ SA-β-gal^+ cells) from total ECs ($Cd45^-Ter119^-CD31^+$ SA-β-gal^- cells) enumerated by fluorescence-activated cell-sorting analysis. (**I**) Relative levels of p16 mRNA expression in liver measured by RT-PCR. Values are shown as mean ± SEM. *P* values in (B) to (F) and (H) and (I) were derived from one-way ANOVA and Tukey posttests. $^*P < 0.05$; $^{**}P < 0.01$; $^{***}P < 0.001$; *P* values > 0.05 are not indicated.

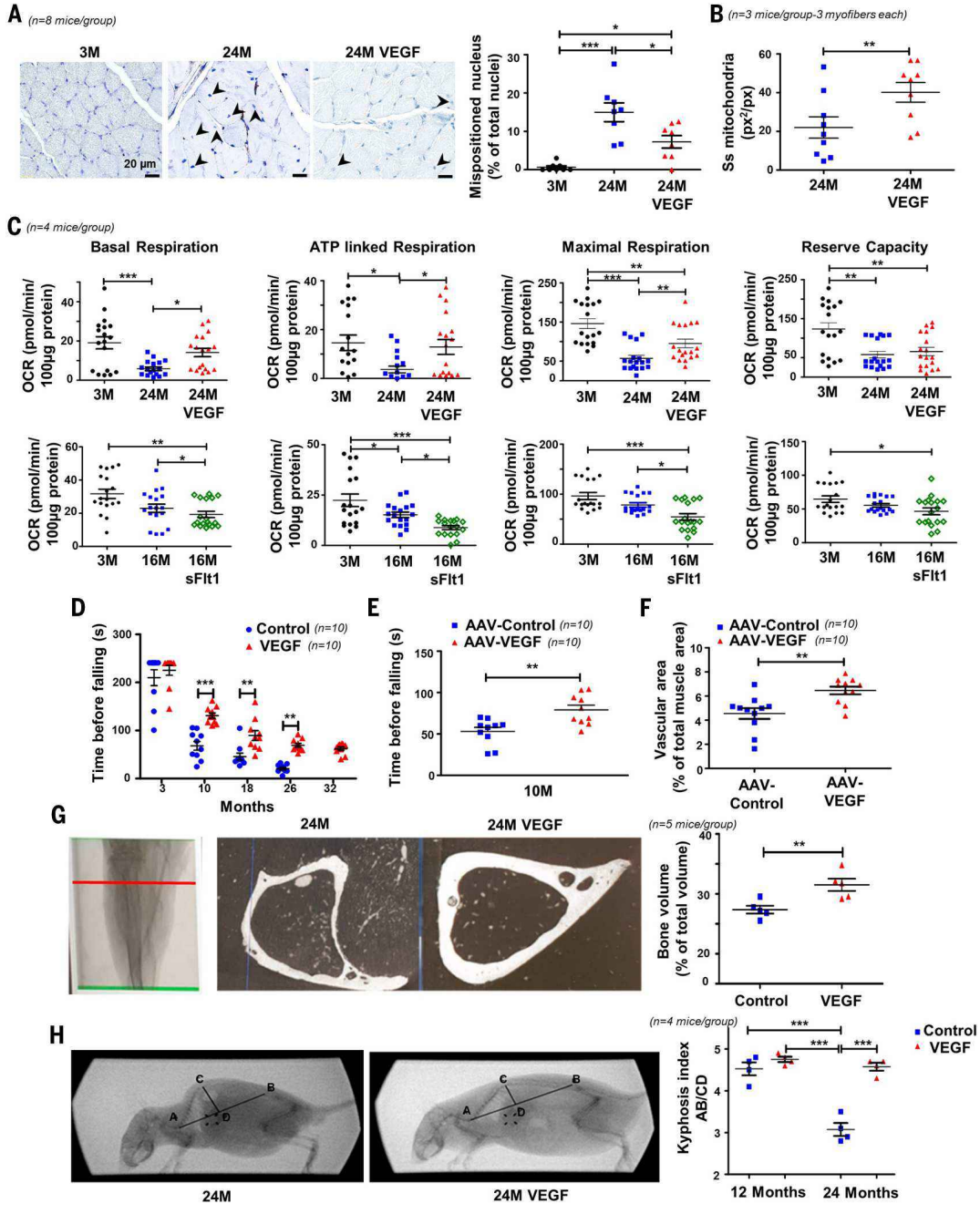

Fig. 4. Alleviation of sarcopenia and osteoporosis in old VEGF-treated mice. (**A**) Left: representative H&E–stained sections of hindlimb muscle showing mispositioned, centrally located nuclei (arrowheads) in muscle fibers of 24 Mo control mice but rarely in 3 Mo or 24 Mo VEGF mice. Right: fraction of centrally located nuclei measured in three sections for each mouse. (**B**) Density of subsarcolemmal mitochondria (Ss), determined as the relative area in a sarcolemma segment occupied by Ss. (**C**) OCR measured ex vivo in myofibrils isolated from hindlimb muscle using a Seahorse platform and normalized to total protein content. Each dot represents pooled myofibers isolated from a mouse (compiled from four independent experiments). (**D**) Mice of the indicated ages were tested for the time that they were able to stay on a rotating rod. (**E**) Rotarod analysis performed on mice preinfected with AAV-VEGF or with AAV-control. (**F**) MVDs in muscle of the same mice used in (E). (**G**) Left: representative micro-CT bone images of hindlimb tibias of 24 Mo female control and VEGF littermates. Images shown are a transverse view at the level marked on the left with a red line. Right: bone volumes calculated and expressed as the fraction of total area occupied by bone. (**H**) Representative images of whole-body x-rays of 24 Mo male control and VEGF littermates. Kyphosis indices were measured from x-ray images in mice of the indicated ages. Values are shown as mean ± SEM. *P* values were derived from one-way ANOVA and Tukey posttest [(A) to (C) and (H)] or two-tailed unpaired Student's *t* test [(D) to (G)]. **P* < 0.05; ***P* < 0.01; ****P* < 0.001; *P* values > 0.05 are not indicated.

VEGF for each mouse used in longevity measurements are provided in tables S1 to S4.

Unlike in most other life span–prolonging interventions characterized by a rightward shift of a sigmoidal curve, VEGF mice (particularly females) presented an atypical survival curve distinguished by its "rectangularization," reflecting that most VEGF mice were still alive when their control littermates were all moribund or dead. This apparent compressed morbidity period indicated that, independent of longevity, VEGF mice may have an increased health span.

Age-associated weight gain was significantly lower in VEGF mice and accelerated weight loss typifying moribund mice did not take place in VEGF mice, which maintained a stable weight up to a few weeks before their death (Fig. 2B and fig. S7). Echo-magnetic resonance imaging (echo-MRI)–based analysis of fat-to-lean body mass ratio indicated that the fat gain observed during the second year of life in control mice was reduced in age-matched VEGF mice of either sex (Fig. 2C and fig. S8).

Carbohydrate utilization and respiratory quotient (RQ) were much higher in VEGF mice (Fig. 2D and fig. S9). The choice of substrates used for energy production at old age correlates with a substrate preference toward lipids, reflecting a reduced capacity for carbohydrate oxidation (*19*). VEGF treatment significantly improved flexibility in substrate usage in old age, as also evidenced by the higher dynamic circadian changes in RQ (fig. S10). A similar metabolic phenotype was observed in an independent, non-transgenic

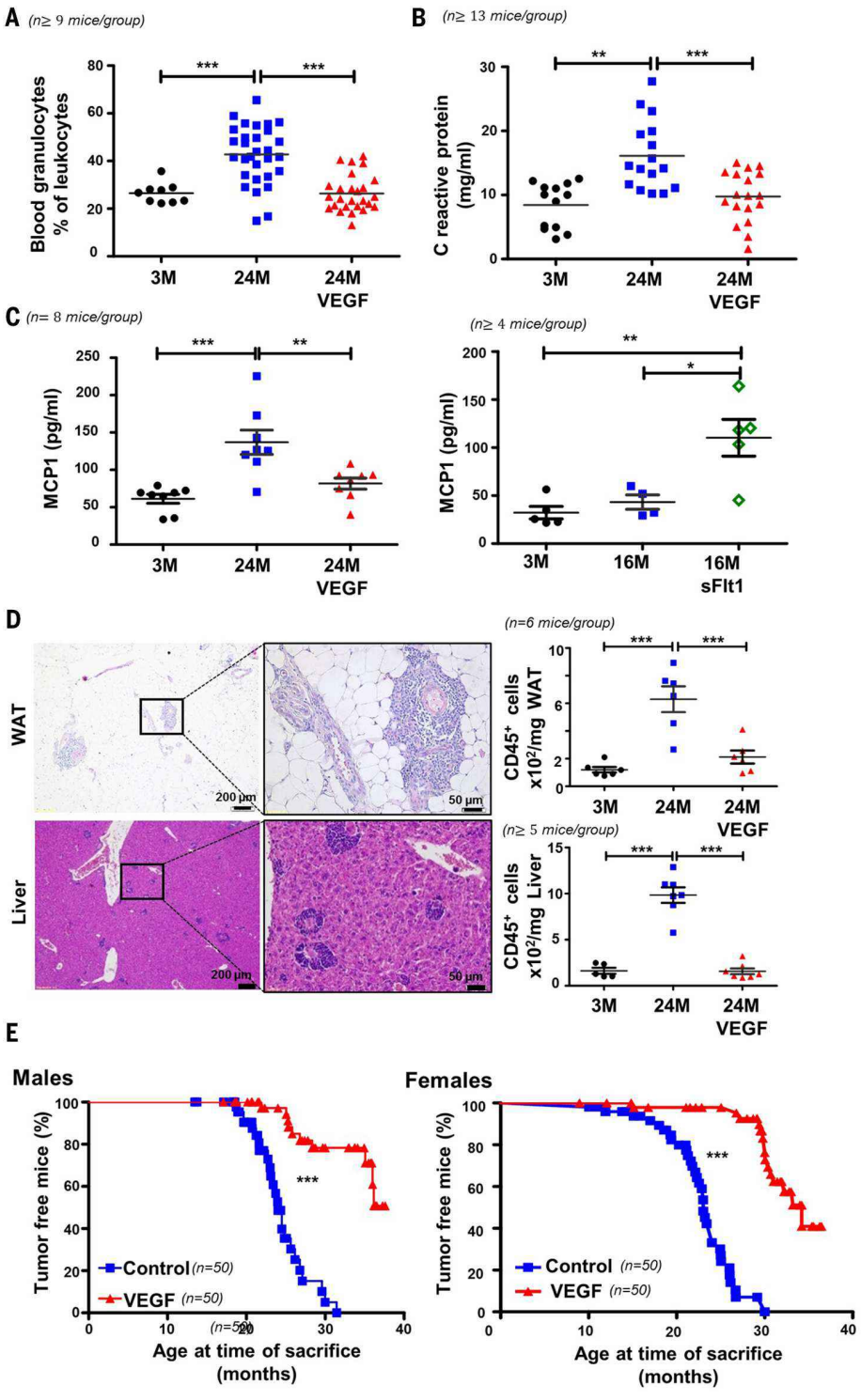

Fig. 5. Inflammaging and tumorigenesis alleviated in VEGF-treated mice. (**A**) Blood granulocytes in mice of the indicated ages calculated as a percentage of total leukocyte counts. (**B**) CRP levels in blood of mice of the indicated ages. (**C**) MCP1 levels in blood of control and VEGF mice (left) and of 16 Mo mice and age-matched sFlt1 mice (right). (**D**) Left: representative images of H&E–stained WAT and liver sections from 18 Mo control mice. Note multiple foci of perivascular and perinecrotic immune cell infiltrates (boxed areas enlarged). Right: $CD45^+$ immune cells in WAT and liver of mice of the indicated ages and genotypes. (**E**) Percentage of animals remaining spontaneously tumor free at sacrifice in control and VEGF mice. Values are shown as mean ± SEM. *P* values were derived from one-way ANOVA and Tukey posttest [(A) to (D)] or log-rank (Mantel-Cox) test (E). $*P < 0.05$; $**P < 0.01$; $***P < 0.001$; *P* values > 0.05 are not indicated.

VEGF gain-of-function system based on adeno-associated virus (AAV)–mediated $VEGF_{164}$ delivery. A low titer of $VEGF_{164}$-encoding AAV (AAV-VEGF) was used, yielding the targeted level of 150 to 200 pg/ml (fig. S11) (i.e., a level comparable to the one attained in the transgenic platform). Increased carbohydrate oxidation and a significantly higher RQ were observed using two different time frames for AAV injections: (i) at the age of 2 months with the metabolic phenotype examined 6 months later (Fig. 2E) or (ii) at the age of 8 months with examination 2 months later (fig. S12).

The observed metabolic changes were not associated with differences in food and water intakes except that aged control mice ate significantly less than younger mice (fig. S13). Although wheel running was not significantly different between control and VEGF mice, total distance covered, reflecting both voluntary and nonvoluntary activities, was higher in male mice and lower in female mice compared with control littermates (fig. S14). Whereas there was no significant difference in daily total energy expenditure (TEE) at 12 months of age (fig. S15) or at 16 months of age between control and VEGF males (Fig. 2F), aged-matched VEGF female mice had a significantly higher TEE than their controls (fig. S16). The basis for these apparent sexual dimorphisms in physical activity and daily TEE is unknown.

Next, we investigated the potential for energy expenditure through thermogenesis, i.e., heat production by uncoupling protein 1 (UCP1)–mediated mitochondrial uncoupling. Because thermogenesis mostly takes place in interscapular brown adipose tissue (BAT), we examined age-associated changes in BAT histology. A higher BAT mass was observed in 24 Mo control mice (fig. S17) but was mostly composed of large white-like adipocytes that had undergone whitening indicative of lost thermogenic capacity. By contrast, BAT in 24 Mo VEGF mice maintained a classic histology of activated BAT characterized by smaller, multi-vacuolated adipocytes (Fig. 2G). Likewise, thermogenic UCP1-expressing beige adipocytes interspersed in white adipose tissue (WAT) were frequently observed in 24 Mo VEGF mice but not in 24 Mo control mice (Fig. 2G).

VEGF treatment ameliorates adverse age-associated alterations in adipose tissue and liver

Aging is usually accompanied by an increase in visceral fat deposition and by a decrease in subcutaneous fat, and both processes are associated with negative health outcomes (*20*). Progressive fat accumulation in the abdominal cavity of control mice and reduced aging-associated fat accumulation in VEGF mice were directly visualized using MRI (Fig. 3A) and were further validated by weighing visceral

WAT harvested at sacrifice (Fig. 3B). Protection from loss of subdermal fat was evidenced by counting more layers of subcutaneous adipocytes in skin sections of 24 Mo VEGF mice compared with control littermates (Fig. 3C).

Aging generally correlates with progressive accumulation of fat within hepatocytes (liver steatosis), a condition predisposing older persons to hepatocyte injury and severe liver pathologies (*21*). Inspection of liver sections from 24 Mo mice, highlighting lipid droplets by Oil Red O staining, revealed that, in contrast to the highly steatotic liver of control littermates, lipid deposition in hepatocytes was greatly reduced in VEGF mice, in which the degree of steatosis resembled more closely that measured in 3 Mo mice (Fig. 3D). Conversely, VEGF loss of function by premature sFlt1 induction led to aggravation of liver steatosis (Fig. 3E). Inspection of liver sections by electron microscopy (EM) corroborated reduced deposition of lipid droplets in old VEGF mice livers and revealed additional adverse alterations reduced by VEGF treatment (fig. S18). Reduced liver injury in 24 Mo VEGF mice was reflected in reduced serum levels of the liver enzymes alanine transaminase and aspartate transaminase (Fig. 3F).

Because liver steatosis has been linked to hepatic senescence (*22*), we examined liver sections stained for senescence-associated β-galactosidase (SA-β-gal) activity. SA-β-gal activity in the livers of old control mice was mostly associated with sinusoidal BVs and only rarely with hepatocytes (Fig. 3G). Quantification of SA-β-Gal$^+$/CD31$^+$ double-positive cells in liver cell suspensions revealed that senescent ECs had accumulated in the aged liver. VEGF reduced the fraction of senescent ECs such that by 2 years of age, VEGF mice had senescent ECs comparable in number to those in 6 Mo control mice (Fig. 3H). Consistent with these results, hepatic p16 expression was up-regulated in the livers of 24 Mo control mice but greatly reduced in the livers of age-matched VEGF mice (Fig. 3I).

VEGF treatment protects from age-related loss of muscle and bone

Aging is associated with progressive loss of skeletal muscle mass and in reduced muscle force–generating capacity (sarcopenia). Because age-related loss of muscle mass in rodents is much lower than that in humans, with only ~15% loss at mean life span (*23*), we examined other anatomical features typifying old muscle (*24*). Mispositioned, centrally located nuclei, reflecting a postinjury muscle response in aged and diseased muscles, were frequently observed in hindlimb muscles of 24 Mo control mice but significantly less so in muscles of VEGF-treated littermates (Fig. 4A). Inspection of muscle sections by EM revealed additional anatomical features frequently observed in muscles of 24 Mo control mice but less frequently in muscles of 24 Mo VEGF mice (fig. S19). Subsarcolemmal-localized mitochondria, which were previously shown to contribute to exercise-induced muscular function improvement (*25*), were more abundant in muscle fibers of old VEGF mice (Fig. 4B and fig. S19).

To evaluate the functional significance of structural mitochondrial alterations in muscle, oxygen consumption rates (OCRs) in young and old muscles were compared using a Seahorse platform. Results showed that myofibrils isolated from skeletal muscle of 24 Mo VEGF mice had significantly higher basal and maximal respiration rates and a higher rate of ATP production than myofibrils isolated from age-matched controls. Conversely, myofibrils isolated from skeletal muscle of 16 Mo sFlt1-induced mice had significantly lower OCR than their control littermates (Fig. 4C). To evaluate differences in force-generating capacity, mice at progressive ages were subjected to a rotarod analysis. Results showed that aging VEGF mice stayed on the rotating rod significantly longer than age-matched controls, with 32 Mo VEGF mice performing as well as control mice half their age (Fig. 4D). Improved rotarod performance was similarly observed using AAV-mediated VEGF delivery to wild-type mice. The 10 Mo mice that were infected with AAV-VEGF 2 months earlier could hold onto a rotating rod 49% longer than their mock-infected littermates could (Fig. 4E). Improved rotarod performance was associated with increased MVD in the muscle of AAV-VEGF–treated mice (Fig. 4F).

Bone weakening caused by bone tissue loss (osteoporosis) is the most common cause of bone breakage in older persons, especially postmenopausal women. Imaging the tibias of 24 Mo female mice by microcomputed tomography (micro-CT) showed that the substantial bone thinning observed in old control mice was reduced in old VEGF mice who had, on average, 33% more bone than control littermates (Fig. 4G).

Age-related alterations in muscle and bone are often manifested in kyphosis, which can be measured from x-ray images: 24 Mo VEGF mice had a 38% higher kyphosis index (i.e., lower outward curve of the spine) than their control littermates (Fig. 4H).

VEGF treatment reduces "inflammaging" and spontaneous tumor burden

"Inflammaging," or age-related multiorgan chronic inflammation, is a fundamental hallmark of aging (*26*). An elevated fraction of granulocytes among circulating leukocytes, indicative of ongoing inflammation, was observed in most old control mice examined but not in age-matched VEGF mice (Fig. 5A). Likewise, longitudinal measurements of the inflammation marker C-reactive protein (CRP) in blood serum showed that, unlike age-matched controls, 24 Mo VEGF mice presented low CRP levels comparable to those detected in 3 Mo mice (Fig. 5B). Monocyte chemoattractant protein-1 (MCP-1), also recognized as a frailty marker (*27*) and validated here to be up-regulated in blood of 24 Mo control mice, was barely elevated in age-matched VEGF mice (Fig. 5C). Conversely, sFlt1 induction led to accelerated MCP-1 accumulation in blood by the age of 16 months (Fig. 5C). Reduced inflammaging in old VEGF mice was also evidenced by the lower number of histologically discernable perivascular inflammatory infiltrates, fewer foci of necrotic inflammation, and a reduced number of infiltrated CD45-positive immune cells enumerated in single-cell suspensions of liver and WAT (Fig. 5D).

Fewer VEGF mice presented one or more neoplastic lesions compared with age-matched control mice when examined at sacrifice (Fig. 5E). The most abundant tumors included lymphomas, lung adenocarcinomas, hepatocellular carcinomas, lipomas, and fibromas (tables S1 and S2). This finding eliminated the concern that transgenic VEGF at the doses used herein may enhance tumorigenesis. Whether there is a causal relationship between reduced inflammaging, a trait recognized as a major tumor promoter (*28*), and reduced tumor burden in old VEGF mice remains to be determined.

Discussion

Aging-associated processes take place at different levels of the biological hierarchy, not just at the cellular level but also at the level of the organ support systems, where vascular aging appears to play a major role. Placing vascular aging in a hierarchically high position in organ aging, as was previously suggested (*3*), is strongly supported by our findings that VEGF-assisted preservation of a young-like vascular homeostasis alleviates key cellular aging hallmarks and age-associated pathologies and, conversely, that premature VEGF neutralization accelerates aging-associated phenotypes. Our data suggest the following sequence of events: increased production of inhibitory VEGF decoy receptors leads to VEGF signaling insufficiency and a resultant failure to maintain adequate MVD. Microvascular deficit, in turn, leads to compromised perfusion, reduced tissue oxygenation, compromised mitochondrial activity, and metabolic alterations. Metabolically active organs, such as the adipose tissue, skeletal muscles, and liver, then progressively lose function and, in the cases of bone and subcutaneous adipose tissue, this is accompanied by significant tissue loss. Therefore, a small increase in circulating VEGF counteracts many adverse processes. This suggests that securing proper

vascular homeostasis during aging might confer a comprehensive geroprotection, i.e., alleviation of major age-related pathologies such as age-associated weight gain, hepatic steatosis, osteoporosis, inflammaging, and increased tumor burden. Further studies might reveal additional organ systems that benefit from VEGF and/or vascular manipulations.

VEGF supplementation resulted in increased longevity of VEGF mice. It is difficult to compare the magnitude of life-span extension obtained by VEGF treatment with that attained by other anti-aging manipulations given the relatively short life span of the mixed mouse strain used in this study (originating from a BALB/cOlaHsd and C57BL/6J crossing) compared with other C57BL/6J–derived strains. In fact, it has been argued that life-span–extending manipulations may remedy deficiencies in the genetic makeup or in the environment of one particular strain rather than altering the aging process (*29*). A non-genetic experimental factor that could have affected longevity was the presence of low-dose tetracycline included in the drinking water.

Although the angiogenic activity of VEGF plays a critical role in the phenotypes observed in this study by virtue of securing adequate perfusion, it is possible that non-angiogenic functions of VEGF play additional geroprotective roles. For example, insufficient VEGF signals were shown to cause a closure of EC fenestrations (*30*) that, when taking place for example in endocrine organs, is bound to impair systemic hormone distribution. VEGF activity also functions in vascular permeability and acts on nonvascular cells (e.g., immune cells) expressing cognate VEGF receptors. As an example, monocytes impair arteriogenesis in aged mice through sFlt1 production (*31*).

We observed increased production of systemic VEGFR1 (sVEGFR1) caused by an age-related shift in the alternative splicing of VEGFR1 mRNA. Alterations in splicing patterns occur frequently in aging (*32*), and it will be of interest to identify the splicing factors responsible for the age-related shift in VEGFR1 mRNA splicing. Additional mechanisms contributing to reduced VEGF signaling in aging might include impaired HIF1 activation and a blunted hypoxic VEGF responsiveness (*33*).

Because the increased levels of systemic VEGF in the mice studied here were in effect from 8 months (corresponding to a human age of 40 years) onward, the VEGF-induced anti-aging effects described should be viewed as preventive in nature. Whether VEGF treatments could be harnessed for reversing established aging phenotypes remains to be investigated. A correlation between VEGF regulation and age-related human pathologies and longevity was also suggested by human studies of polymorphisms in the VEGF gene promoter region (*34*).

This study demonstrates that perturbation of microvascular homeostasis is a critical driving force in multiorgan aging. Correspondingly, it suggests that harnessing VEGF-aided restoration of vascular homeostasis may serve as a method for inducing a multifaceted increase in health span.

Methods summary

A transgenic Tet-off system was used for liver-specific, conditional VEGF-A_{164} induction in mice originating from a BALB/cOlaHsd and C57BL/6J crossing, producing modestly elevated levels of circulatory VEGF from early adulthood onward. A comparable level of VEGF (150 to 200 pg/ml of plasma) was attained using AAV-assisted VEGF delivery to naive mice. For VEGF loss of function, transgenic sVEGFR1 was conditionally induced using an EC-specific driving transgene. VEGF and sVEGFR1 serum levels were monitored using VEGF and VEGFR1 enzyme-linked immunosorbent assay (ELISA) and VEGF signaling by measuring the fraction of VEGFR2 phosphorylation from total VEGFR2. Phenotypic longitudinal analyses performed in control and manipulated mice littermates included the following: MRI-based measurements of the fat-to-lean ratio; ultrasound photoacoustics measurement of tissue oxygenation; x-ray bone visualization and micro-CT measurements of bone volume; OCR measurements in isolated muscle fibers using a Seahorse platform; rotarod analysis for measuring muscle-generating force; metabolic analysis, TEE, and physical activity measured in metabolic cages; endothelial senescence quantified by measuring SA-β-gal activity in sorted ECs; inflammaging evaluated by leukocyte infiltration and by measuring inflammation markers in blood; and tumor burden evaluated by visual inspection at sacrifice. Reverse transcription polymerase chain reaction (RT-PCR), EM, and immunohistochemistry were performed using standard methods. GraphPad Prism version 7 software was used for statistical analysis. A detailed account of the methods used in this study is provided in the supplementary materials.

REFERENCES AND NOTES

1. S. Rafii, J. M. Butler, B. S. Ding, Angiocrine functions of organ-specific endothelial cells. *Nature* **529**, 316–325 (2016). doi: 10.1038/nature17040; pmid: 26791722
2. Z. Ungvari *et al.*, Endothelial dysfunction and angiogenesis impairment in the ageing vasculature. *Nat. Rev. Cardiol.* **15**, 555–565 (2018). doi: 10.1038/s41569-018-0030-z; pmid: 29795441
3. D. G. Le Couteur, E. G. Lakatta, A vascular theory of aging. *J. Gerontol. A Biol. Sci. Med. Sci.* **65**, 1025–1027 (2010). doi: 10.1093/gerona/glq135; pmid: 20650862
4. B. J. North, D. A. Sinclair, The intersection between aging and cardiovascular disease. *Circ. Res.* **110**, 1097–1108 (2012). doi: 10.1161/CIRCRESAHA.111.246876; pmid: 22499900
5. M. S. Goligorsky, Microvascular rarefaction: The decline and fall of blood vessels. *Organogenesis* **6**, 1–10 (2010). doi: 10.4161/org.6.1.10427; pmid: 20592859
6. A. P. Kusumbe, S. K. Ramasamy, R. H. Adams, Coupling of angiogenesis and osteogenesis by a specific vessel subtype in bone. *Nature* **507**, 323–328 (2014). doi: 10.1038/nature13145; pmid: 24646994
7. Y. Hasegawa *et al.*, Blockade of the nuclear factor-κB pathway in the endothelium prevents insulin resistance and prolongs life spans. *Circulation* **125**, 1122–1133 (2012). doi: 10.1161/CIRCULATIONAHA.111.054346; pmid: 22302838
8. A. Das *et al.*, Impairment of an endothelial NAD^+-H_2S signaling network is a reversible cause of vascular aging. *Cell* **173**, 74–89.e20 (2018). doi: 10.1016/j.cell.2018.02.008; pmid: 29570999
9. S. Tarantini *et al.*, Nicotinamide mononucleotide (NMN) supplementation rescues cerebromicrovascular endothelial function and neurovascular coupling responses and improves cognitive function in aged mice. *Redox Biol.* **24**, 101192 (2019). doi: 10.1016/j.redox.2019.101192; pmid: 31015147
10. M. B. Chen *et al.*, Brain endothelial cells are exquisite sensors of age-related circulatory cues. *Cell Rep.* **30**, 4418–4432.e4 (2020). doi: 10.1016/j.celrep.2020.03.012; pmid: 32234477
11. A. J. Barinda *et al.*, Endothelial progeria induces adipose tissue senescence and impairs insulin sensitivity through senescence associated secretory phenotype. *Nat. Commun.* **11**, 481 (2020). doi: 10.1038/s41467-020-14387-w; pmid: 31980643
12. A. Lazarus, E. Keshet, Vascular endothelial growth factor and vascular homeostasis. *Proc. Am. Thorac. Soc.* **8**, 508–511 (2011). doi: 10.1513/pats.201102-021MW; pmid: 22052928
13. A. S. Maharaj, M. Saint-Geniez, A. E. Maldonado, P. A. D'Amore, Vascular endothelial growth factor localization in the adult. *Am. J. Pathol.* **168**, 639–648 (2006). doi: 10.2353/ajpath.2006.050834; pmid: 16436677
14. D. May *et al.*, Transgenic system for conditional induction and rescue of chronic myocardial hibernation provides insights into genomic programs of hibernation. *Proc. Natl. Acad. Sci. U.S.A.* **105**, 282–287 (2008). doi: 10.1073/pnas.0707778105; pmid: 18162550
15. T. Licht *et al.*, VEGF preconditioning leads to stem cell remodeling and attenuates age-related decay of adult hippocampal neurogenesis. *Proc. Natl. Acad. Sci. U.S.A.* **113**, E7828–E7836 (2016). doi: 10.1073/pnas.1609592113; pmid: 27849577
16. K. Furrer *et al.*, Serotonin reverts age-related capillarization and failure of regeneration in the liver through a VEGF-dependent pathway. *Proc. Natl. Acad. Sci. U.S.A.* **108**, 2945–2950 (2011). doi: 10.1073/pnas.1012531108; pmid: 21282654
17. T. Takahashi, S. Yamaguchi, K. Chida, M. Shibuya, A single autophosphorylation site on KDR/Flk-1 is essential for VEGF-A-dependent activation of PLC-gamma and DNA synthesis in vascular endothelial cells. *EMBO J.* **20**, 2768–2778 (2001). doi: 10.1093/emboj/20.11.2768; pmid: 11387210
18. R. L. Kendall, K. A. Thomas, Inhibition of vascular endothelial cell growth factor activity by an endogenously encoded soluble receptor. *Proc. Natl. Acad. Sci. U.S.A.* **90**, 10705–10709 (1993). doi: 10.1073/pnas.90.22.10705; pmid: 8248162
19. C. E. Riera, A. Dillin, Tipping the metabolic scales towards increased longevity in mammals. *Nat. Cell Biol.* **17**, 196–203 (2015). doi: 10.1038/ncb3107; pmid: 25720959
20. J. L. Kuk, T. J. Saunders, L. E. Davidson, R. Ross, Age-related changes in total and regional fat distribution. *Ageing Res. Rev.* **8**, 339–348 (2009). doi: 10.1016/j.arr.2009.06.001; pmid: 19576300
21. I. H. Kim, T. Kisseleva, D. A. Brenner, Aging and liver disease. *Curr. Opin. Gastroenterol.* **31**, 184–191 (2015). doi: 10.1097/MOG.0000000000000176; pmid: 25850346
22. M. Ogrodnik *et al.*, Cellular senescence drives age-dependent hepatic steatosis. *Nat. Commun.* **8**, 15691 (2017). doi: 10.1038/ncomms15691; pmid: 28608850
23. S. B. Ballak, H. Degens, A. de Haan, R. T. Jaspers, Aging related changes in determinants of muscle force generating capacity: A comparison of muscle aging in men and male rodents. *Ageing Res. Rev.* **14**, 43–55 (2014). doi: 10.1016/j.arr.2014.01.005; pmid: 24495393
24. R. K. Sayed *et al.*, Identification of morphological markers of sarcopenia at early stage of aging in skeletal muscle of mice. *Exp. Gerontol.* **83**, 22–30 (2016). doi: 10.1016/j.exger.2016.07.007; pmid: 27435496
25. E. V. Menshikova *et al.*, Effects of exercise on mitochondrial content and function in aging human skeletal muscle. *J. Gerontol. A Biol. Sci. Med. Sci.* **61**, 534–540 (2006). doi: 10.1093/gerona/61.6.534; pmid: 16799133
26. S. Salvioli *et al.*, Inflamm-aging, cytokines and aging: State of the art, new hypotheses on the role of mitochondria and new perspectives from systems biology. *Curr. Pharm. Des.* **12**,

3161–3171 (2006). doi: 10.2174/138161206777947470; pmid: 16918441
27. M. J. Yousefzadeh *et al*., Circulating levels of monocyte chemoattractant protein-1 as a potential measure of biological age in mice and frailty in humans. *Aging Cell* **17**, e12706 (2018). doi: 10.1111/acel.12706; pmid: 29290100
28. G. C. Leonardi, G. Accardi, R. Monastero, F. Nicoletti, M. Libra, Ageing: From inflammation to cancer. *Immun. Ageing* **15**, 1 (2018). doi: 10.1186/s12979-017-0112-5; pmid: 29387133
29. B. G. Hughes, S. Hekimi, Different mechanisms of longevity in long-lived mouse and *Caenorhabditis elegans* mutants revealed by statistical analysis of mortality rates. *Genetics* **204**, 905–920 (2016). doi: 10.1534/genetics.116.192369; pmid: 27638422
30. D. May *et al*., A transgenic model for conditional induction and rescue of portal hypertension reveals a role of VEGF-mediated regulation of sinusoidal fenestrations. *PLOS ONE* **6**, e21478 (2011). doi: 10.1371/journal.pone.0021478; pmid: 21779329
31. G. Zhao *et al*., The soluble VEGF receptor sFlt-1 contributes to impaired neovascularization in aged mice. *Aging Dis.* **8**, 287–300 (2017). doi: 10.14336/AD.2016.0920; pmid: 28580185
32. K. Wang *et al*., Comprehensive map of age-associated splicing changes across human tissues and their contributions to age-associated diseases. *Sci. Rep.* **8**, 10929 (2018). doi: 10.1038/s41598-018-29086-2; pmid: 30026530
33. S. Rey, G. L. Semenza, Hypoxia-inducible factor-1-dependent mechanisms of vascularization and vascular remodelling. *Cardiovasc. Res.* **86**, 236–242 (2010). doi: 10.1093/cvr/cvq045; pmid: 20164116
34. R. Del Bo *et al*., Role of VEGF gene variability in longevity: A lesson from the Italian population. *Neurobiol. Aging* **29**, 1917–1922 (2008). doi: 10.1016/j.neurobiolaging.2007.05.003; pmid: 17574707

ACKNOWLEDGMENTS

We thank R. Hertz, J. Bar-Tana, S. Ben-Sasson, and Y. Dor for helpful discussions; T. Oliven and D. Maimoun for technical help; D. Agrawal and V. Krizhanovsky for technical help with the SA-β-gal assay; D. Kushnir (Surgical Innovation and Technology Center, Hadassah Medical Center) for help with x-ray imaging; T. Lifschytz and B. Lerer from the National Knowledge Center for Research on Brain Disorders (Hadassah Medical Center) for help with the rotarod performance assay; and A. Grunewald for artwork. **Funding:** This work was supported in part by research grants from the Britain Israel Research and Academic Exchange partnership (BIRAX grant no. 58BX18MMEK), the Israel Science Foundation (grant nos. 783/20 and 2779/19), the Novo Nordisk Foundation (grant no. NNF16C0023554), The Sigrid Jusélius Foundation, and the Hospital District of Helsinki. K.A. was supported by a Uusimaa Research Grant. **Author contributions:** M.G., S.K., H.S., E.V., A.G.H., T.L., M.H., and S.L. performed experiments. A.P., L.H., S.A., and J.T. performed metabolic analyses. R.A. performed MRI and perfusion analysis. Y.F. performed EM imaging. A.A. and K.A. provided AAV-VEGF and AAV-control viruses. O.Z.K., R.H., and V.D. performed part of the bone density analysis. R.T. and P.K. provided technical assistance and performed data analysis. M.G. and E.K. conceptualized the study, designed experiments, interpreted data, wrote the manuscript, and supervised the study. **Competing interests:** M.G. and E.K. are inventors on a patent entitled "Anti-aging compositions and methods of use" (US provisional application no. 62/656,471). The remaining authors declare no competing interests. **Data and materials availability:** All data are available in the main text or the supplementary materials.

SUPPLEMENTARY MATERIALS

science.sciencemag.org/content/373/6554/eabc8479/suppl/DC1
Materials and Methods
Figs. S1 to S19
Tables S1 to S4
References (*35*–*43*)
MDAR Reproducibility Checklist

View/request a protocol for this paper from *Bio-protocol*.

18 May 2020; resubmitted 19 January 2021
Accepted 6 June 2021
10.1126/science.abc8479

Science

Counteracting age-related VEGF signaling insufficiency promotes healthy aging and extends life span

M. Grunewald, S. Kumar, H. Sharife, E. Volinsky, A. Gileles-Hillel, T. Licht, A. Permyakova, L. Hinden, S. Azar, Y. Friedmann, P. Kupetz, R. Tzuberi, A. Anisimov, K. Alitalo, M. Horwitz, S. Leebhoff, O. Z. Khoma, R. Hlushchuk, V. Djonov, R. Abramovitch, J. Tam and E. Keshet

Science **373** (6554), eabc8479.
DOI: 10.1126/science.abc8479

More VEGF, more life span and health span

Advanced aging is celebrated but its ill effects of deterioration at the cell, tissue, and organ levels are not. Grunewald *et al.* provide evidence for the vascular theory of aging, which reports that an age-related decrease of vascular function is a driver of organismal aging at large (see the Perspective by Augustin and Kipnis). Vascular endothelial growth factor (VEGF) signaling insufficiency underlies this vascular insufficiency in aged mice. A modest compensatory increase in circulatory VEGF was sufficient to preserve a young-like vascular homeostasis, alleviate multiple adverse age-related processes, and ameliorate a host of age-associated pathologies in mice.

Science, abc8479, this issue p. eabc8479; see also abj8674, p. 490

Science (print ISSN 0036-8075; online ISSN 1095-9203) is published by the American Association for the Advancement of Science, 1200 New York Avenue NW, Washington, DC 20005. The title *Science* is a registered trademark of AAAS.